AMERICAN SOCIETY FOR MICROBIOLOGY | mSphere®

RESEARCH ARTICLE
Host-Microbe Biology

# Two *Verticillium dahliae* MAPKKKs, VdSsk2 and VdSte11, Have Distinct Roles in Pathogenicity, Microsclerotial Formation, and Stress Adaptation

**Jun Yu,[a] Tianyu Li,[a] Longyan Tian,[a] Chen Tang,[a] Steven J. Klosterman,[b] Chengming Tian,[a] Yonglin Wang[a]**

[a]Beijing Key Laboratory for Forest Pest Control, College of Forestry, Beijing Forestry University, Beijing, China
[b]Agricultural Research Service, U.S. Department of Agriculture, Salinas, California, USA

**ABSTRACT** *Verticillium dahliae* causes destructive vascular wilt diseases on more than 200 plant species, including economically important crops and ornamental trees worldwide. The melanized microsclerotia enable the fungus to survive for years in soil and are crucial for its disease cycle. Previously, we found that the VdPbs2-VdHog1 (*V. dahliae* Pbs2-*V. dahliae* Hog1) module plays key roles in microsclerotial formation, stress responses, and virulence in *V. dahliae*. In this study, two mitogen-activated protein kinase kinase kinases (MAPKKKs) homologous to Ssk2p and Ste11p, which activate the Pbs2p-Hog1p module by phosphorylation in budding yeast, were identified in the genome of *V. dahliae*. Both Δ*VdSsk2* (*V. dahliae Ssk2*) and Δ*VdSte11* strains showed severe defects in microsclerotial formation and melanin biosynthesis, but the relative importance of these two genes in microsclerotial development was different. Deletion of *VdSsk2*, but not *VdSte11*, affected responses to osmotic stress, fungicidal response, and cell wall stressors. The Δ*VdSsk2* strain exhibited a significant reduction in virulence, while the Δ*VdSte11* strain was nonpathogenic due to failure to penetrate and form hyphopodia. Phosphorylation assays demonstrated that VdSsk2, but not VdSte11, can phosphorylate VdHog1 in *V. dahliae*. Moreover, *VdCrz1*, encoding a calcineurin-responsive zinc finger transcription factor and a key regulator of calcium signaling in fungi, was misregulated in the Δ*VdSsk2*, Δ*VdPbs2*, and Δ*VdHog1* mutants.

**IMPORTANCE** These data provide insights into the distinctive functions of VdSsk2 and VdSte11 in pathogenicity, stress adaptation, and microsclerotial formation in *V. dahliae*.

**KEYWORDS** MAPKKK, *Verticillium dahliae*, microsclerotia, pathogenicity, stress response

*Verticillium dahliae* is a soilborne fungus that infects more than 200 dicotyledonous plant species and causes devastating vascular wilt diseases (1). The resting structures of this fungus are known as microsclerotia, which generate infectious hyphae that penetrate the host epidermis directly and colonize the root cortex. After a brief period in the cortex, the fungus enters the xylem tissue (2). As vascular colonization and wilt development progresses, *V. dahliae* produces melanized microsclerotia in dying plant tissues, representing new primary inocula (3). Melanin deposition is tightly coupled with microsclerotial development (4), though it is not required for pathogenicity (5). However, melanin does provide protection from UV irradiation and temperature extremes (5), enzymatic lysis, nutrient deprivation, and fungicidal activities (6). Thus, melanized microsclerotia are vital to the survival of this pathogen in soil, sometimes for very long periods, in the absence of a host plant. Because of their vitally important roles in the life cycle and disease spread, microsclerotia are considered important targets for

**Citation** Yu J, Li T, Tian L, Tang C, Klosterman SJ, Tian C, Wang Y. 2019. Two *Verticillium dahliae* MAPKKKs, VdSsk2 and VdSte11, have distinct roles in pathogenicity, microsclerotial formation, and stress adaptation. mSphere 4: e00426-19. https://doi.org/10.1128/mSphere.00426-19.

**Editor** Aaron P. Mitchell, Carnegie Mellon University



Address correspondence to Yonglin Wang, ylwang@bjfu.edu.cn.

J.Y., T.L., and L.T. contributed equally to this work.

**Received** 13 June 2019
**Accepted** 24 June 2019
**Published** 10 July 2019

disease control (4, 7). Therefore, elucidation of the molecular mechanisms that underlie microsclerotial development and pathogenicity, including the key signaling pathways that control these processes, represent important steps in the quest for novel control strategies.

Mitogen-activated protein kinase (MAPK) cascades, as key cores of signaling networks in fungi and other eukaryotes, mediate the signaling required to initiate infection-related morphogenesis and for a variety of cellular adaptations to diverse stimuli (8). To activate the MAPK cascade, a MAPK kinase kinase (MAPKKK) phosphorylates the MAPK kinase (MAPKK), which in turn activates the MAPK by phosphorylation. The high-osmolarity glycerol (Hog) pathway is one of the MAPK signaling pathways that is activated by deleterious environmental conditions, such as high osmolarity, citric acid, and heat stresses (9). This pathway is well understood in the yeast *Saccharomyces cerevisiae* (9, 10). The canonical Hog pathway contains two branches, mediated by Sho1p and Sln1p, which converge on the MAPKK Pbs2p (11, 12). Two MAPKKKs, Ste11p and Ssk2p/Ssk22p, activate the Pbs2p-Hog1p module in *S. cerevisiae* (13).

The core components of the Hog pathway are well conserved in fungi, and their biological roles in regulating stress adaptation have been reported in several filamentous plant-pathogenic fungi, such as *Magnaporthe oryzae*, *Cryphonectria parasitica*, *Botrytis cinerea, Mycosphaerella graminicola*, and the oomycete *Phytophthora sojae* (14–19). Systematic characterization of the kinome of plant pathogen *Fusarium graminearum* revealed that *F. graminearum* Ssk22 (FgSsk22) functions upstream of FgPbs2 and FgOs2 (20), indicating that it is different from yeast somehow. However, our knowledge about upstream MAPKK and MAPKKKs in filamentous fungi is more limited.

Calcium ($Ca^{2+}$) signaling is also involved in fungal development and stress tolerance (21). After binding $Ca^{2+}$, the protein calmodulin activates calcineurin (22). Crz1 (calcineurin-responsive zinc finger) is an important downstream transcription factor, whose function is dependent on appropriate $Ca^{2+}$ signaling in fungi (23). For example, *M. oryzae* CRZ1 (MoCRZ1) is essential for tolerance to ion stress, maintaining cell wall integrity, and virulence in *M. oryzae* (24, 25). In *B. cinerea*, the CRZ1 homolog is required for sclerotial formation and pathogenicity (26).

In recent years, some of the key components of signal transduction in *V. dahliae* have been characterized, including those of MAPK pathways (VMK1, VdMsb, VdSho1, VdPbs2, VdHog1, and VdMsn2) (27–31), and VdCrz1 (32). Vmk1 was the first characterized MAPK in *V. dahliae*, and it is an ortholog of yeast Kss1p, which is required for filamentous growth in *S. cerevisiae* (33). Vmk1 is essential for pathogenicity, though the *vmk1* mutant is also defective in conidiation and microsclerotial formation (31). *V. dahliae* mutants lacking the transmembrane mucin, VdMsb, exhibit significant reductions in invasive growth, adhesive capacity, conidiation, and microsclerotial formation (34). VdSho1 controls external sensing, virulence, and multiple growth-related traits in *V. dahliae* (30). Previously, the kinase module VdPbs2-VdHog1 has been functionally characterized in *V. dahliae* (28, 29). Yet the roles of upstream MAPKKKs VdSsk2 and VdSte11, which are conserved and thought to signal to the Hog MAP kinase cascade, are not well understood in *V. dahliae*.

The objective of this current study was to confirm or establish functional similarities in signaling, if any, between VdSsk2 and VdSte11, as upstream MAPKKKs, and secondarily to determine whether these kinases contribute to virulence in *V. dahliae*. In this study, we have characterized the roles of VdSsk2 and VdSte11 in signal transduction in *V. dahliae*. Overall, our data indicate that *V. dahliae* differs from the model yeasts in the lack of convergence of both Ssk2p and Ste11p on the Hog pathway, and this supports a model whereby only VdSsk2 acts upstream of the VdPbs2-VdHog1 module. VdSsk2 is a major regulator of some stress responses analyzed, and VdSte11 is essential for pathogenicity and melanin biosynthesis. Through genetic analyses, we discovered that VdSsk2 and VdSte11 have distinctive functions in microsclerotial formation and that the calcineurin-responsive zinc finger transcription factor VdCrz1 acts downstream of the Hog MAPK pathway through $Ca2^{+}$ signaling. These findings clarify functional relation-

ships of key upstream components of signaling pathways that govern virulence, microsclerotial development, and stress responses in *V. dahliae*.

## RESULTS

***VdSte11* affects hyphal morphology in *V. dahliae*.** MAPKKKs homologous to yeast Ssk2/Ssk22p and Ste11p were identified in the genome of *V. dahliae*. The two genes, *VdSsk2* (*V. dahliae Ssk2*) and *VdSte11*, encode proteins that share high identity to the yeast proteins Ssk2p and Ste11p, respectively. The yeast has two kinases, Ssk2p and Ssk22p, whereas *V. dahliae* has only VdSsk2. VdSsk2 and VdSte11 are also highly homologous to other Ssk2p and Ste11p orthologs from other fungi, respectively (see Fig. S1 and S2 in the supplemental material). To functionally investigate the roles of *VdSsk2* and *VdSte11*, three independent deletion mutants were obtained for each gene and verified by multiple PCR analyses and DNA blots (Fig. S3). Mutants were complemented by introduction of the wild-type copies of either *VdSsk2* or *VdSte11* into the mutant strains (Fig. S3).

Phenotypic observations of the Δ*VdSsk2* and Δ*VdSte11* strains revealed no major growth defects on various media (Fig. S4). However, the colonies of the Δ*Vdste11* strain appeared smooth and exhibited less aerial mycelia than the colonies of other strains (Fig. S4). After incubation on basal medium (BM), aerial mycelial growth was markedly reduced in the Δ*VdSte11* strain versus the Δ*VdSsk2* strain, the complemented strains, and wild-type strain XS11 (Fig. 1A). The germ tubes from the conidia of the Δ*VdSte11* strain were convoluted with disproportionate branching and septation relative to the other strains, appearing near yeast-like in growth at 24 and 48 h postinoculation (hpi). Furthermore, the mycelial clumps of the Δ*VdSte11* strain that formed in the liquid 7 days postinoculation (dpi) were strikingly smaller than the wild-type strain XS11 and the Δ*VdSsk2* strain (Fig. 1B). After staining with calcofluor white (CFW), the Δ*VdSte11* strain exhibited enhanced hyphal compartmentalization relative to other strains (Fig. 1C, red arrowheads). The mean number of hyphal septa of the Δ*VdSte11* strain was 1.5 times more than that of other strains (Fig. 1D). Given these findings above, we concluded that VdSte11 plays an essential role in filamentous growth over solid surfaces and in liquid media, while VdSsk2 has no obvious effect on filamentous growth and morphology.

***VdSsk2* and *VdSte11* play distinct roles in microsclerotial formation and melanin biosynthesis.** To investigate functions of *VdSsk2* and *VdSte11* in microsclerotial formation, we first assessed the ability of the above strains to form microsclerotia on different media, such as potato dextrose agar medium (PDA), BM, and complete medium (CM). Microscopic examination showed that the Δ*VdSte11* andΔ*VdSsk2* strains produced less melanized microsclerotia compared to wild-type strain XS11 and the complemented strains (Fig. 2A, B, and C). Interestingly, deletion of *VdSte11* led to more severe defect in melanization. Further observations and quantification demonstrated that the Δ*VdSsk2* strain produced melanized microsclerotia in significantly reduced numbers (five times less than strain XS11), while the Δ*Vdste11* strain produced smaller microsclerotia that were devoid of the pigmentation characteristic of melanin deposition (Fig. 2D). Strikingly, swollen hyphal clusters (microsclerotial initials) abundantly appeared amid the colonies of the Δ*Vdste1* strain. Quantification of microsclerotia revealed that the Δ*Vdste11* strain produced clusters about 1.3 times more than strain XS11 did (Fig. 2E). Even at 60 dpi, while the Δ*VdSsk2* strain formed similar sized melanized microsclerotia similar to those observed in strain XS11, the Δ*Vdste11* strain produced fewer melanized microsclerotia, which were also smaller than those of the other strains examined (Fig. S5). These results indicated that both VdSsk2 and VdSte11 participate in microsclerotium formation, but the roles of the two are distinctive. That is, VdSsk2 affects the number of melanized microsclerotia, while VdSte11 regulates melanin production or deposition during microsclerotial development.

To determine how VdSsk2 and VdSte11 affect the expression patterns of genes with known roles in melanin biosynthesis or those previously shown as highly upregulated

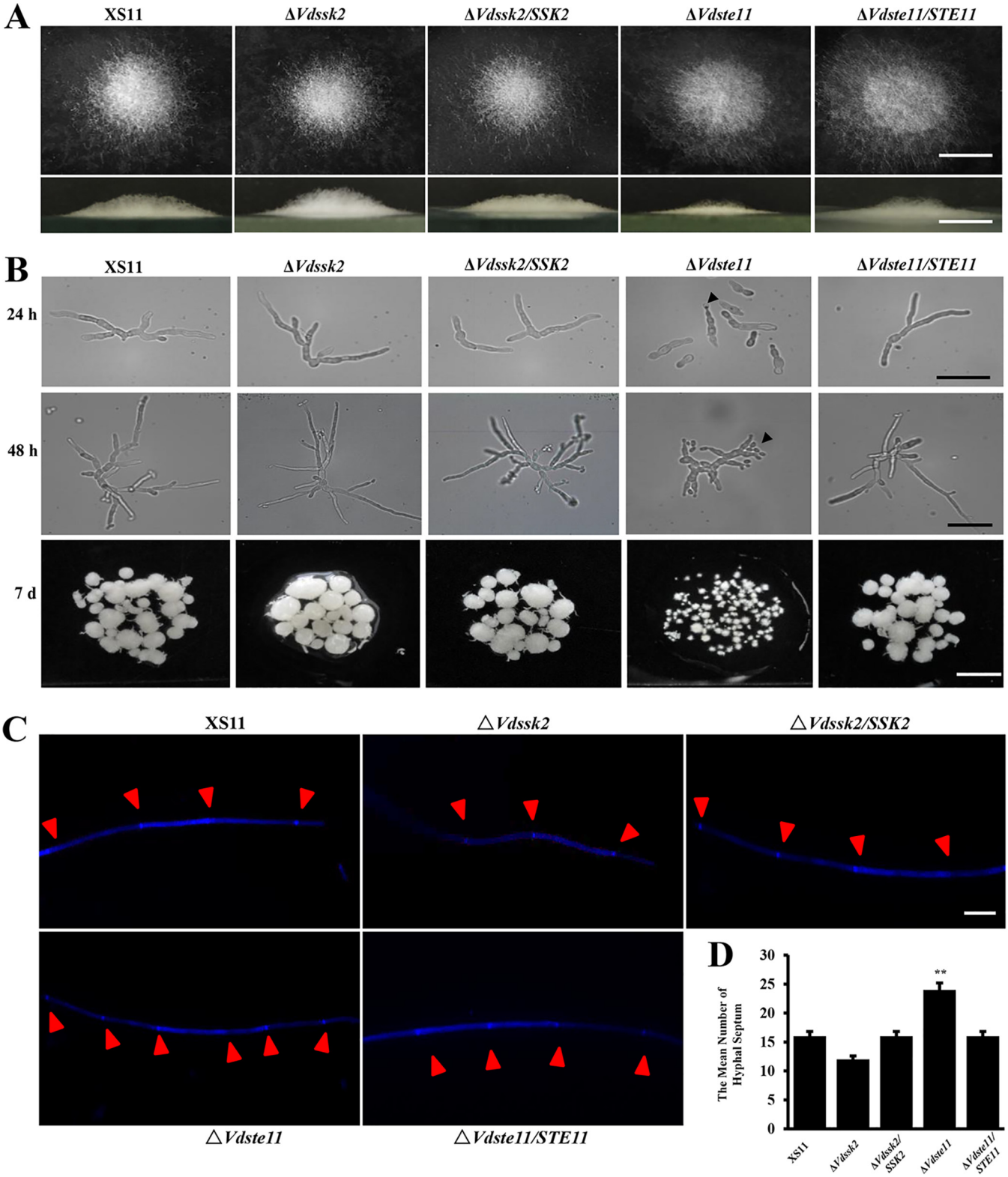


**FIG 1** The phenotypes of Δ*VdSsk2* and Δ*VdSte11* strains of *Verticillium dahliae* in axenic culture. (A, top) Colony morphology of XS11, Δ*VdSsk2*, and Δ*VdSte11* strains, and the respective complemented strains were incubated on BM for 7 days. The aerial hyphal growth of the strains was observed after growth. (Bottom) Vertical dissection of the colonies. Bars = 1 cm. (B) Strains were cultured in yeast extract peptone-dextrose liquid medium at 25°C for 24 h, 48 h, and 7 days (d). Germination of conidia and filamentous branching were imaged with a compound microscope. All cultures were inoculated with the same amount of spores ($10^6$ conidia/ml). Bars = 0.5 cm. (C) Strains were cultured on PDA for 7 days. Germ tubes from germinated conidia and hyphae were stained with 10 mg/ml CFW for 5 min. The CFW signal was imaged by fluorescence microscopy, and the CFW signal in the hyphal septum was quantified separately. Bar = 10 $\mu$m. (D) Number of hyphal septum calculated in the single hypha in panel C. Values are means plus standard deviations (error bars) from three replicates. Values that are significantly different ($P < 0.01$) from the value for the wild-type strain XS11 are indicated by two asterisks.

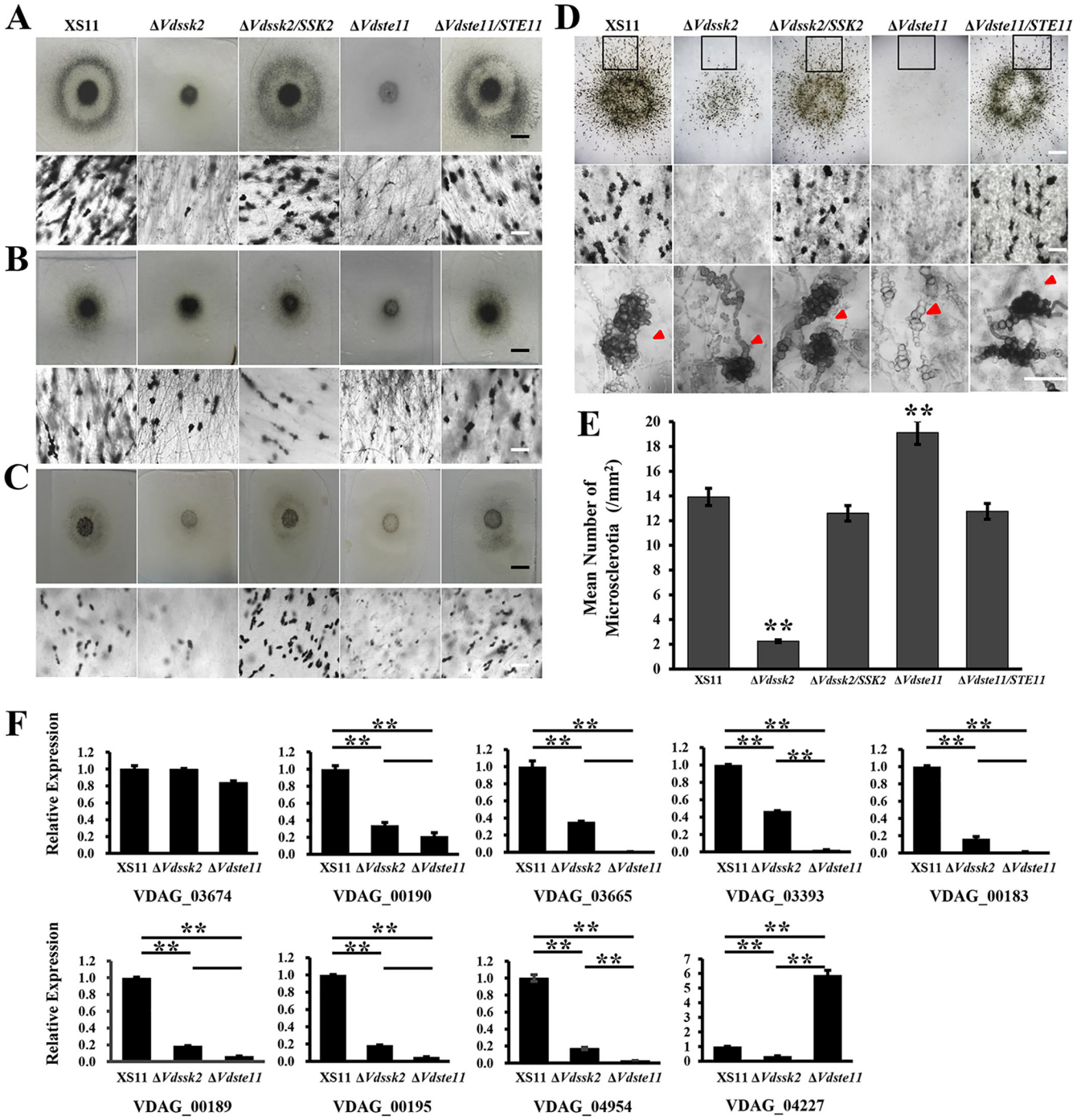


**FIG 2** Distinct roles of *VdSsk2* and *VdSte11* in the formation of melanized microsclerotia in *Verticillium dahliae*. (A to C) Microscopic examination of the colonies of XS11, Δ*VdSsk2,* and Δ*VdSte11* strains and complemented strains cultured on PDA (A), BM (B), and CM (C) at 25°C for 7 days. The top panels show colonies observed with a dissection microscope (bar = 0.5 cm). The bottom panels represent melanized microsclerotial formation with a dissection microscope (bar = 40 $\mu$m). (D) The microsclerotial formation of the above strains in detail was observed after the strains were cultured on BM at 25°C for 10 days. The top panels represent the whole view of microsclerotial formation (bar = 0.5 cm). The middle and bottom panels show microsclerotial formation of the black squares in the top panel in more enlarged views at different magnifications (bars = 40 $\mu$m). Images were taken by using a microscope. Red arrowheads indicate immature or melanized microsclerotia. (E) Mean number of microsclerotia or hyphal cell aggregation calculated from the black squares in the top panels of Fig. 2B. Error bars represent standard deviations of three replicates, and asterisks represent significant differences ($P < 0.01$). (F) Relative expression level of nine known genes related with melanin biosynthesis in *V. dahliae*. RNAs were extracted from the mycelia incubated on PDA for 7 days at 25°C. Error bars represent standard deviations of three replicates, and asterisks represent significant differences ($P < 0.01$). There were two biological experiments performed for each strain and three technical replicates per biological experiment.

**TABLE 1** Known and putative melanin biosynthetic genes of *Verticillium dahliae*[a]

| Gene ID/name in *V. dahliae* | Function | Reference |
|---|---|---|
| VDAG_03674 | Acetyl-CoA carboxylase | 4 |
| VDAG_00190/*VdPks1* | Polyketide synthase | 4 |
| VDAG_03665/*VdBrn1* | Tetrahydroxynaphthalene reductase | 4 |
| VDAG_03393/*VdScd1* | Scytalone dehydratase | 4 |
| VDAG_00183/*VdBrn2* | Versicolorin reductase | 4 |
| VDAG_00189/*VdLac1* | Laccase | 5 |
| VDAG_00195/*VdCmr1* | Transcription factor Pig1 | 5 |
| VDAG_04954/*Vayg1* | Polyketide chain shortening | 67 |
| VDAG_04227/*VdMsn2* | $C_2H_2$ transcription factor | 27 |

[a]Names and functions of the genes tested in qPCRs. CoA, coenzyme A.

during melanin biosynthesis (4, 5, 7). Reverse transcription-quantitative PCR (RT-qPCR) analyses were performed on the gene sets (Table 1): *VDAG_03674*, *VdPks1* (*VDAG_00190*), *VdBrn1* (*VDAG_03665*), *VdScd1* (*VDAG_03393*), *VdBrn2* (*VDAG_00183*), *VdLac1* (*VDAG_00189*), *VdCmr1* (*VDAG_00195*), *Vayg1* (*VDAG_04954*), and *VdMsn2* (*VDAG_04227*). Consistent with a deficiency in melanization during culturing, gene expression data showed that seven genes, including *VdPKS1*, *VdLac1*, and *VdCmr1*, were significantly downregulated in both the *VdSsk2* and *VdSte11* mutants (Fig. 2F), suggesting that both VdSsk2 and VdSte11 positively regulate the expression of genes involved in melanin biosynthesis. However, the expression levels of these genes in the Δ*Vdste11* strain were much lower than that of the Δ*VdSsk2* mutant (Fig. 2F), indicating that VdSte11 functions as a major regulator of melanin biosynthesis and is further consistent with the phenotype of the Δ*VdSte11* strain. However, the transcript levels of *VDAG_03674* observed in both mutants were not significantly different from those of strain XS11. The expression of *VdMsn2* (*VDAG_04227*), which is a negative regulator of melanized microsclerotial formation (27), was obviously downregulated in the Δ*VdSsk2* strain but significantly upregulated in the Δ*VdSte11* strain. This strengthened the idea that VdSte11 might play a major role in melanin biosynthesis in *V. dahliae*. Collectively, we concluded that VdSsk2 and VdSte11 have overlapping functions in regulating some melanin biosynthetic genes, but their roles are different in melanin biosynthesis and microsclerotial development, suggesting the participation in different signaling pathways in *V. dahliae*.

**Deletion of *VdSte11* impairs penetration, whereas deletion of *VdSsk2* affects fungal proliferation.** To determine the roles of *VdSsk2* and *VdSte11* in virulence, we performed pathogenicity assays on tobacco seedlings by root dip inoculation with conidial suspensions ($2 \times 10^6$ conidia/ml) from each mutant strain, complemented strains, and wild-type strain XS11. At 35 dpi, pathogenicity assays showed that tobacco seedlings inoculated by the Δ*VdSte11* strain exhibited no chlorosis, while about 40% of seedlings inoculated by the Δ*VdSsk2* strain appeared slightly chlorotic (the yellowing of the leaves in Fig. 3A). In contrast, about 40% of seedlings inoculated with strain XS11 and complemented strains showed severe wilt symptoms (Fig. 3A). Both Δ*VdSsk2* and Δ*VdSte11* mutants displayed significantly reduced disease severity. Figure 3B shows that the Δ*VdSte11* strain was nonpathogenic, and while the Δ*VdSsk2* strain caused typical *Verticillium* wilt symptoms, the disease severity (2 seedlings died, 9 seedlings wilted, and 9 seedlings showed no symptom; $n = 20$ seedlings) was significantly lower than that observed following inoculation with strain XS11 and the complemented strains (Fig. 3B). Correspondingly, fungal hyphae were not recovered from plants inoculated with the Δ*VdSte11* strain, while the Δ*VdSsk2* strain could be reisolated from vascular tissue at a lower rate of isolation than those of the *VdSsk2*-complemented strain and XS11 (Fig. 3C).

To further characterize the defect of the Δ*VdSte11* strain in pathogenicity, we first assayed the penetration of hyphae through the cellophane membrane. On CM overlaid with the cellophane membrane, neither Δ*VdSte11* nor Δ*VdSsk2* strains exhibited obvious defects in colony morphology at 5 dpi, similar to earlier observations recorded on

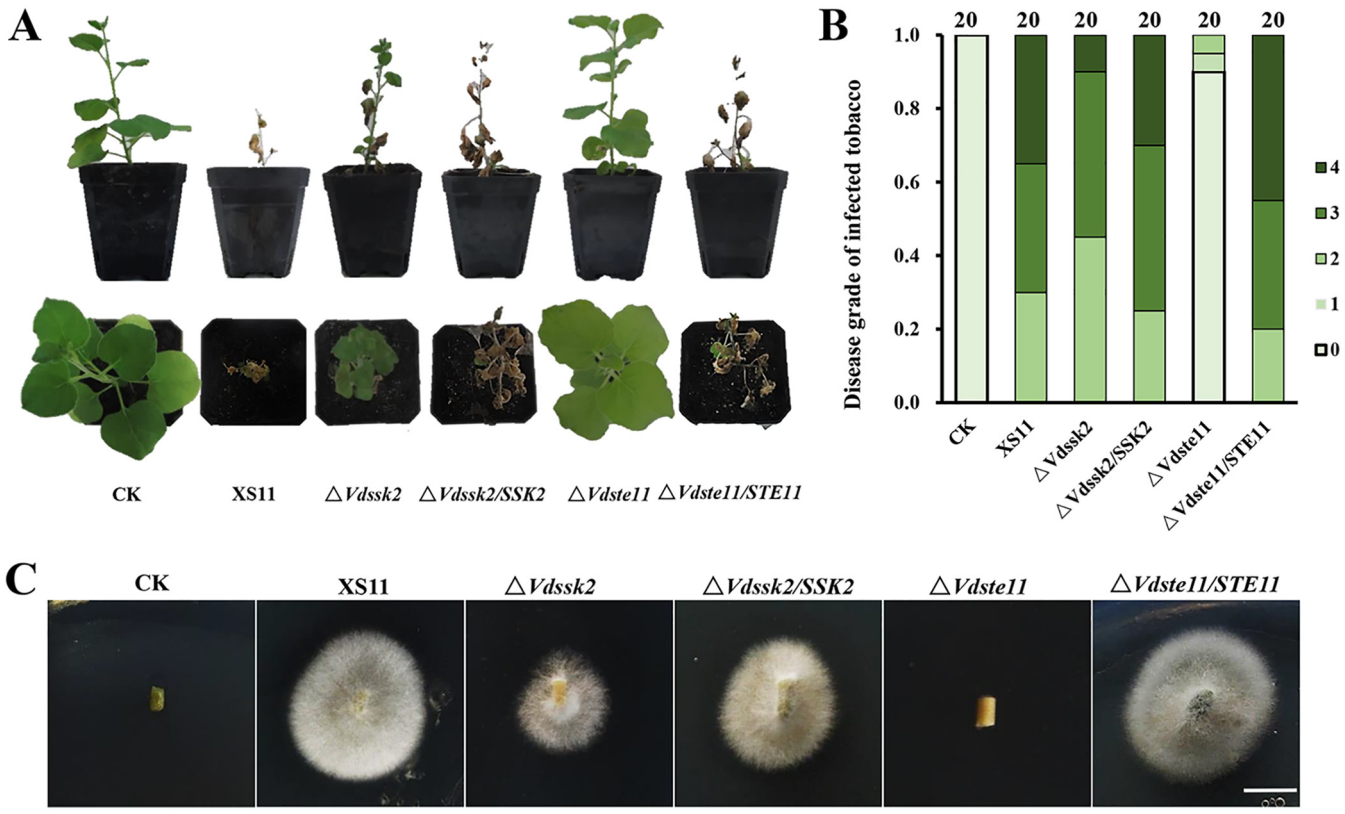


**FIG 3** The *Verticillium dahliae* Δ*VdSsk2* and Δ*VdSte11* strains exhibit severe defects in pathogenicity. (A) Two-month-old tobacco seedlings were inoculated with a conidial suspension ($10^6$ conidia/ml) of XS11 strain, Δ*VdSsk2* and Δ*VdSte11* deletion strains, and complemented strains for 30 min. Control inoculations (CK) were performed by dipping seedlings in distilled water for 30 min. All seedlings were replanted into the soil after root dipping. Photographs were taken at 35 dpi, respectively. (B) Disease levels were scored according to the number of seedlings that showed wilt symptoms or had died. Twenty seedlings were inoculated with each strain. The disease ratings of the symptoms were calculated at 35 dpi. 0 = no wilting, 1 = yellowing or wilting of <2 leaves, 2 = yellowing or wilting of one-fourth leaves, 3 = yellowing or wilting of two-thirds leaves, and 4 = more than 85% of the leaves wilted or the whole plant died. (C) Reisolation of *V. dahliae* strains from the system of inoculated tobacco plants at 25°C for 7 days. Images were taken after transferring fungal colonies from the stem sections to PDA at 25°C for 10 days. Bar indicates 0.5 cm.

PDA. However, the inability of hyphae to penetrate through the cellophane membrane was notable in the Δ*VdSte11* strain, while there was only a slight defect in penetration of hyphae in the Δ*VdSsk2* strain; successful penetration of the wild type and the complemented strains occurred, as visualized after removal of the cellophane membrane at 2 dpi (Fig. 4A). In addition, the Δ*VdSte11* strain failed to form hyphopodia for penetration pegs, whereas the Δ*VdSsk2* strain, strain XS11, and the complemented strains produced abundant hyphopodia on the cellophane membrane (Fig. 4B). Another penetration assay was performed using onion epidermal tissue. The results of this assay showed that the Δ*VdSte11* strain did not penetrate into onion epidermis, since no invasive hyphae (IH) appeared in the Δ*VdSte11* mutant, while infectious hyphae were abundant in Δ*VdSsk2*, XS11, and the complemented strains (Fig. 4C). These results suggest that VdSsk2 and VdSte11 have distinct roles in pathogenesis. In conclusion, deletion of *VdSte11* impairs penetration, whereas deletion of *VdSsk2* affects proliferation in the xylem.

**The Δ*VdSsk2* mutant phenocopies the Δ*VdPbs2* and Δ*VdHog1* mutants under various stressors.** Because deletion of *VdPbs2* and *VdHog1* led to enhanced sensitivity to osmotic stresses (28, 29), we also examined the Δ*VdSsk2* and Δ*VdSte11* strains in relation to osmotic stress to determine whether one of these kinases functions in the same pathway as the VdPbs2-VdHog1 module. Compared with wild-type strain XS11 and the complemented strains, the Δ*VdSsk2* strain exhibited dramatic hypersensitivity to high-osmolarity stresses such as NaCl and sorbitol and increased resistance to fungicides such as fludioxonil and iprodione (Fig. 5A and B), which was consistent with

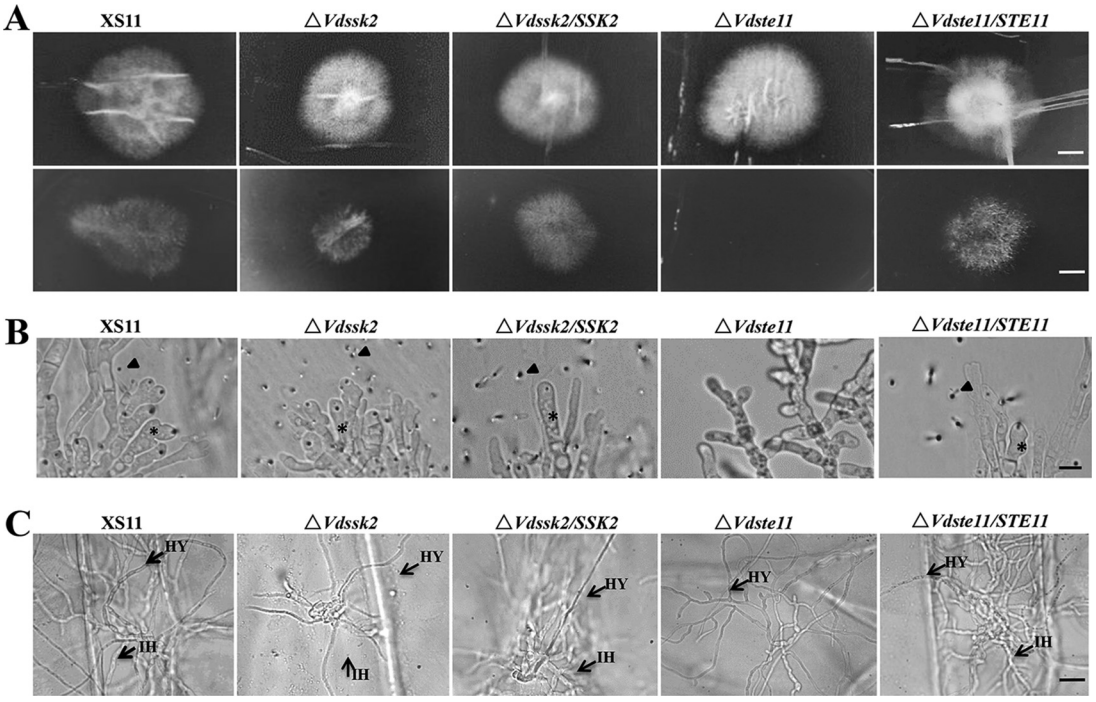


**FIG 4** Penetration and plant infection analyses of the *VdSsk2* and *VdSte11* mutant strains of *Verticillium dahliae*. (A) Cellophane membranes were plated onto minimal medium and inoculated with conidia harvested from wild-type strain XS11, the Δ*VdSsk2* and Δ*VdSte11* strains, and the respective complemented strains. Penetration was examined at 5 dpi. The top panels show colonies of the strain grown on the cellophane membranes covered above PDA at 5 dpi. The bottom panels show colonies grown from hyphae penetrating through the membrane at another 2 dpi after removing cellophane membrane. Bars = 0.5 cm. (B) Hyphopodia and penetration pegs formed on the cellophane membrane by the above strains. Black asterisks and arrowheads indicate hyphopodia and penetration pegs, respectively. The Δ*VdSte11* strain failed to form hyphopodia and penetrate the membrane. Bar = 5 $\mu$m. (C) Infection assays of onion epidermis 48 h after inoculation of strains XS11, Δ*VdSsk2*, Δ*VdSte11*, and the respective complemented strains. Black arrows point to invasive hyphae (IH) and hyphae (HY). Bar = 20 $\mu$m.

previous results obtained by examining the Δ*VdPbs2* and Δ*VdHog1* strains (28, 29). On the other hand, sensitivity of the Δ*Vdste11* strain to the above stresses was comparable to that observed in strain XS11 (Fig. 5A and B).

In addition, we demonstrated that aberrant chitin distribution occurred in the Δ*VdSsk2* strain under osmotic stress compared with wild-type strain XS11 (Fig. 5C). The deletion of *VdSsk2* caused enhanced growth on media with CFW (10, 20, and 30 $\mu$g/ml) and Congo red (CR) (25 $\mu$g/ml) compared with strain XS11, respectively (Fig. 5D). The statistical analyses showed that the Δ*VdSsk2* strain was significantly different from strain XS11 and the Δ*VdSsk2* complementation strains ($P < 0.01$) (Fig. 5E), but the Δ*Vdste11* strain showed no difference from strain XS11 (Fig. 5D and E). Moreover, chitin synthase and $\beta$-1,3-glucan synthase are involved in the synthesis of chitin and $\beta$-1,3-glucan in fungi (35). We identified three genes encoding components involved in cell wall integrity, such as *VDAG_02340*, *VDAG_02341* which encodes 1,3-$\beta$-glucan synthase, and *VDAG_08428* which encodes a glucan synthesis regulatory protein. Figure 5F shows that loss of *VdSsk2* induced significantly higher expression of three genes, indicating that *VdSsk2* negatively regulates chitin synthesis. Taken together, the results demonstrated that the deletion of *VdSsk2*, *VdPbs2,* and *VdHog1*, but not *VdSte11*, caused hypersensitivity to high osmolarity and resistance to fludioxonil, suggesting that VdSsk2 functions in the same signaling pathways as VdPbs2 and VdHog1 in *V. dahliae*.

**The VdSsk2-VdPbs2-VdHog1 signaling pathway is involved in high $Ca^{2+}$ concentration tolerance.** To elucidate the contribution of the VdSsk2-VdPbs2-VdHog1 module plus VdSte11 to adaptation of high $Ca^{2+}$ levels, we tested the tolerance of each mutant to different concentrations of $Ca^{2+}$. The Δ*VdSsk2* strain exhibited increased sensitivity to calcium at higher concentrations, similar to that observed in the Δ*VdCrz1*,

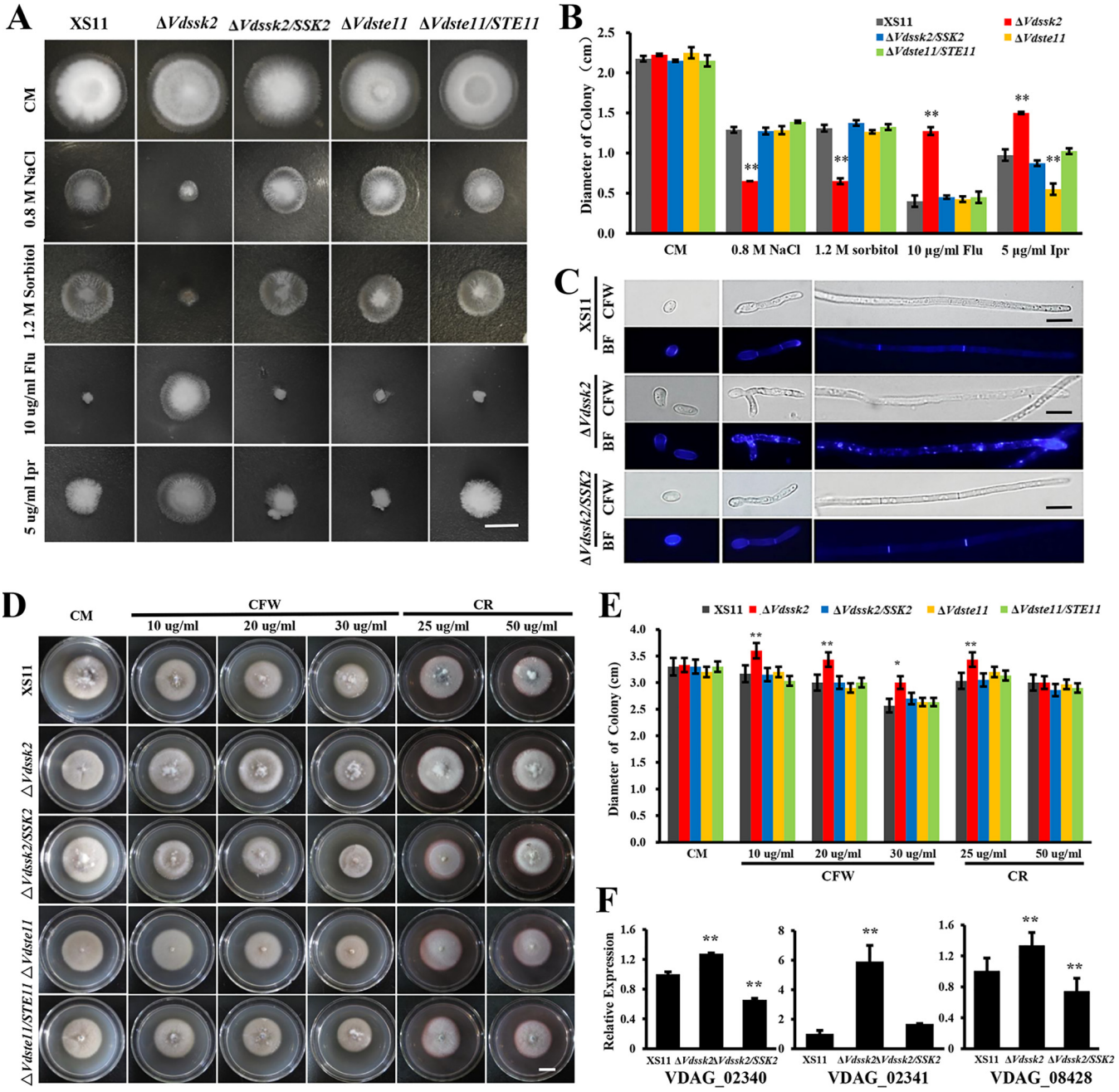


**FIG 5** *VdSsk2* of *Verticillium dahliae* is essential to mount the wild-type response to osmotic agents, fungicides, calcofluor white (CFW), and Congo red (CR). (A) The colony morphology of the wild-type strain XS11, the Δ*VdSsk2* and Δ*VdSte11* strains, and the respective complemented strains grown on complete medium (CM) or CM supplemented with 0.8 M NaCl, 1.2 M sorbitol, 10 μg/ml fludioxonil, and 5 μg/ml iprodione. Photographs were taken at 8 days. Bar = 1 cm. (B) Colony diameters of the indicated strains. Values are means ± standard deviations (error bars) for three replicates, and asterisks show values that are significantly different ($P < 0.01$). (C) Chitin distribution was observed in strain XS11, the Δ*VdSsk2* strain, and the *VdSsk2* complemented strain grown in CM liquid supplemented with 0.6 M NaCl for 4 days. Conidia and hyphae were stained with 10 mg/ml CFW for 5 min. The CFW signal was imaged by fluorescence microscopy, and images were also captured by bright-field microscopy (BF). Bars = 10 μm. (D) The colony morphology of the above XS11 strains were grown on CM containing CFW and CR at 25°C for 5 days. Bar = 0.5 cm. (E) Relative growth inhibition of colonies of each strain. Values are means ± standard deviations (error bars) for three replicates, and asterisks show values that are significantly different ($P < 0.01$). (F) Expression of three genes associated with cell wall biosynthesis was analyzed by RT-qPCR and normalized against the expression of *V. dahliae* β-*tubulin* (7). Values are means plus standard deviations (error bars) for three independent experiments, and asterisks show values that are significantly different ($P < 0.01$).

Δ*VdPbs2*, and Δ*VdHog1* strains (Fig. 6A). Interestingly, the Δ*VdHog1*, Δ*VdPbs2*, and Δ*VdSsk2* strains were more sensitive to higher $Ca^{2+}$ than the Δ*Vdcrz1* mutant. The hyphal growth of the Δ*VdHog1*, Δ*VdPbs2*, and Δ*VdSsk2* strains was approximately 50% of that of the Δ*Vdcrz1* mutant in the presence of 0.4 M $Ca^{2+}$ (Fig. 6B). However, the

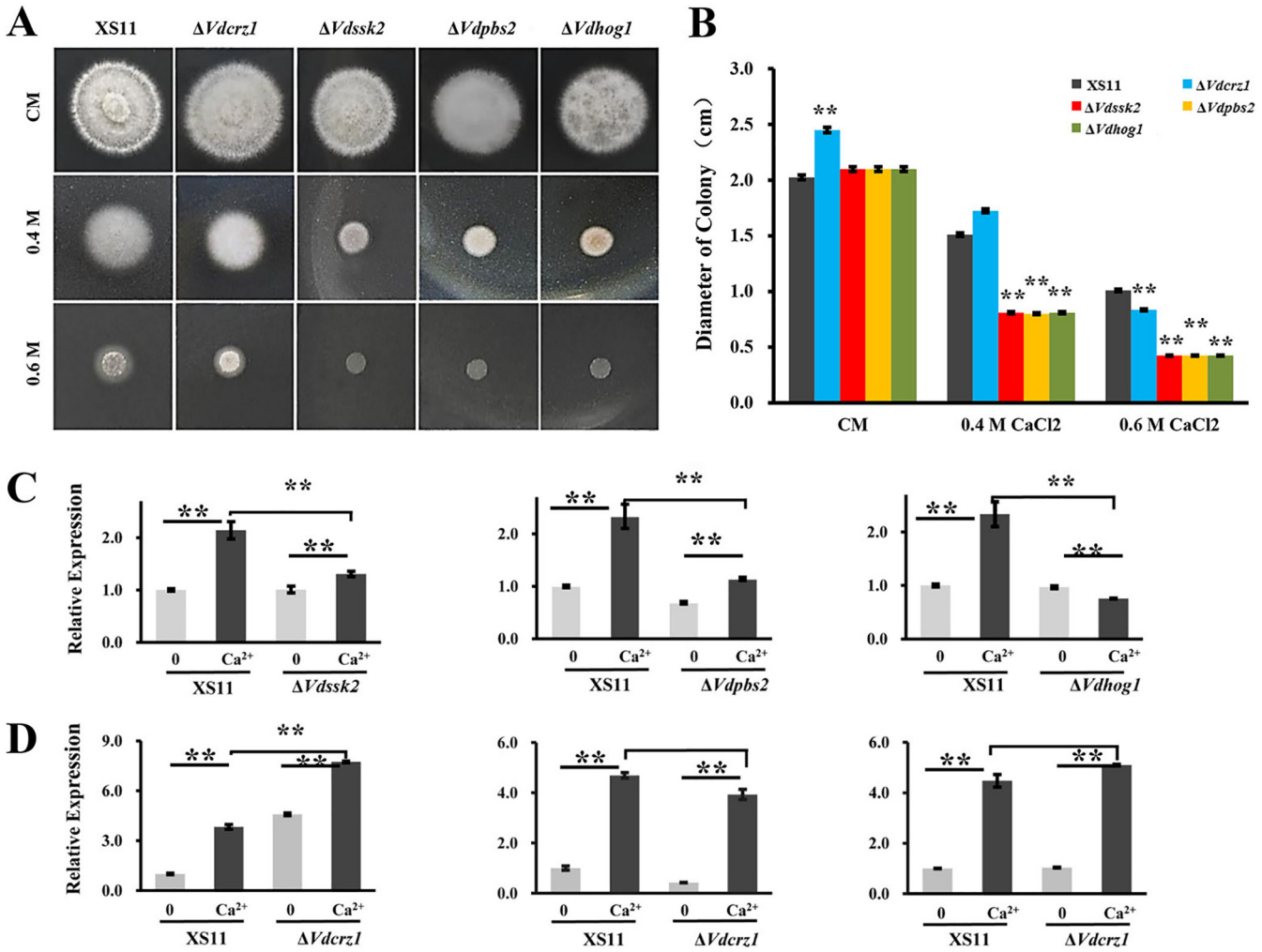


**FIG 6** *VdCrz1* is misregulated in the *VdSsk2*, *VdPbs2*, and *VdHog1* mutant strains of *Verticillium dahliae*. (A) Colony morphology of wild-type strain XS11 and of the Δ*VdSsk2*, Δ*Vdpbs2*, Δ*Vdhog1*, and Δ*Vdcrz1* strains on CM medium with or without $Ca^{2+}$. Strains were grown for 5 days. Bar = 1 cm. (B) Colony diameters of strains. Values are means ± standard deviations (error bars) for three replicates, and asterisks show values that are significantly different ($P < 0.01$). (C) Transcript levels of *VdCrz1* were compared between strain XS11 and the Δ*VdSsk2*, Δ*Vdpbs2*, and Δ*Vdhog1* strains. Strains were grown on CM without $Ca^{2+}$ or with 0.3 M $Ca^{2+}$ for 30 min. Values are means ± standard deviations (error bars) from three independent experiments. (D) The expression levels of *VdSsk2*, *Vdpbs2*, and *Vdhog1* were analyzed in strain XS11 and the Δ*Vdcrz1* strain when grown on CM without $Ca^{2+}$ or with 0.3 M $Ca^{2+}$ for 30 min. Values are means ± standard deviations (error bars) from three independent experiments.

Δ*VdSte11* strain showed sensitivity to higher $Ca^{2+}$ similar to that of strain XS11 (data not shown). Furthermore, we performed expression analyses of *VdCrz1* by RT-qPCR to gain insight into the relationship between *VdCrz1* expression in the genetic background of the Δ*VdHog1*, Δ*VdPbs2*, and Δ*VdSsk2* strains and in the wild-type strain XS11. While the expression levels of *VdCrz1* were significantly higher in response to $Ca^{2+}$ in the XS11 strain, the levels of *VdCrz1* were not altered in any of the three mutants (Fig. 6C), suggesting that *VdCrz1* expression induced by $Ca^{2+}$ is dependent on the Hog MAPK cascade. In contrast, expression levels of three genes (*VdHog1*, *VdPbs2*, and *VdSsk2*) were upregulated by $Ca^{2+}$ regardless of the presence or absence of *VdCrz1* (Fig. 6D), indicating that the Hog MAPK cascade acts upstream of VdCrz1. These findings indicated that expression of *VdCrz1* was at least partially dependent on the VdSsk2-VdPbs2-VdHog1 signaling pathway and that misregulation in the expression of *VdCrz1* in response to $Ca^{2+}$ treatment could account for high $Ca^{2+}$ sensitivity in the Δ*VdHog1*, Δ*VdPbs2*, and Δ*VdSsk2* strains.

**VdSsk2, but not VdSte11, activates VdHog1.** An initial aim of this work was to investigate whether either the MAPKKKs encoded by *VdSsk2* and *VdSte11* could phos-

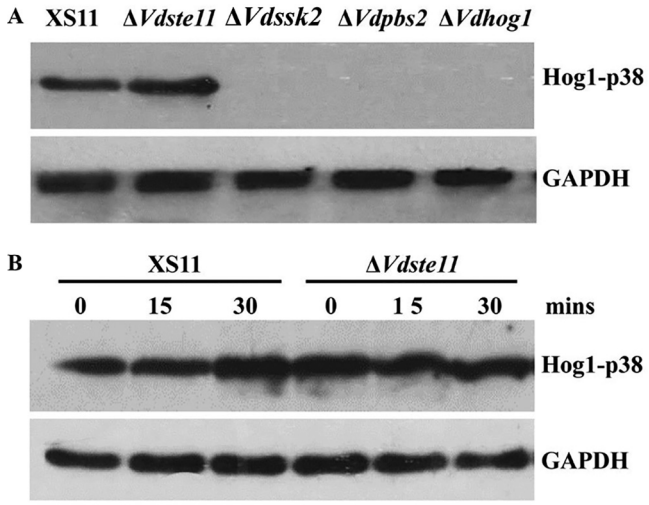


**FIG 7** VdHog1 phosphorylation requires VdSsk2, but not VdSte11, in *Verticillium dahliae*. (A) The phosphorylation levels are shown for VdHog1 in XS11, Δ*VdSte11*, Δ*VdSsk2*, Δ*VdPbs2,* and Δ*VdHog1* strains. All strains were incubated for 3 days in YEPD broth, and total proteins were extracted for immunoblot analysis. (B) VdHog1 activation by NaCl induction. The strains were grown for 3 days and exposed to 0.7 M NaCl in YEPD broth for 15 or 30 min, and total proteins were extracted for immunoblot analysis. The separated total proteins from *V. dahliae* were transferred to a nitrocellulose membrane and the anti-phospho-p38 monoclonal antibody (P-Hog1; Cell Signaling) was used to detect the phosphorylated form of the VdHog1p. The same blots were stripped and then reprobed with GAPDH antibody as an internal control.

phorylate VdHog1. Hog1 phosphorylation was not observed in the Δ*VdSsk2* strain in this study consistent with observations made on the Δ*VdPbs2* strain, but the level of Hog1 phosphorylation in the Δ*VdSte11* mutant was similar to that observed in the wild-type strain (XS11) (Fig. 7A). Induction of Hog1 phosphorylation occurred in the Δ*VdSte11* strain, and this phosphorylation was stimulated by NaCl, similar to that observed in strain XS11 (Fig. 7B). These findings suggested that VdSsk2, but not VdSte11, functions as the upstream activator of the VdPsb2-VdHog1 module in *V. dahliae*.

## DISCUSSION

The Hog MAPK signaling pathway in fungi is important for sensing stressful conditions and the activation of gene expression that enables fungi to resist osmotic stress and to survive under other adverse conditions (13). In *S. cerevisiae*, the two MAPKKKs, Ste11p and Ssk2/Ssk2p, activate the Pbs2p-Hog1p module. However, whether orthologs of Ste11p and Ssk2/Ssk2p converge on Pbs2 has not been conclusively shown in filamentous fungi (8, 9). Several lines of evidence in this current study demonstrate that VdSsk2, but not VdSte11, functions as an integral component of the Hog signaling pathway in *V. dahliae*. First, mutants lacking *VdSsk2* phenocopied *VdPbs2* or *VdHog1* deletion mutants in response to stress treatments. Second, as inferred from discernible microsclerotial formation phenotypes, VdSsk2 and VdSte11 play distinctive roles in melanized microsclerotial formation. Third, the phosphorylation level of *VdHog1* was affected by the deletion of either *VdSsk2* or *VdPbs2*, but not *VdSte11*. Finally, *VdSte11* inactivation in *V. dahliae* resulted in the loss of pathogenicity due to a defect in plant infection, while the *VdSsk2* deletion resulted in attenuated virulence similar to mutants of *VdPbs2* or *VdHog1*.

The data presented herein suggest that the Ste11p MAPKKK ortholog in *V. dahliae* does not activate the Ssk2-Pbs2-Hog1 cascade. This is different from the pattern observed in *S. cerevisiae*, where the Hog1p MAPK is regulated by three functionally redundant MAPKKKs, including Ste11p, Ssk2p, and Ssk2p. In this study, we identified only one kinase (VdSsk2) unlike the two kinases (Ssk2p, and Ssk2p) found in *S. cerevisiae*. The mutant lacking *VdSsk2* resulted in equivalent stress-related phenotypes

as exhibited by the Δ*Vdpbs2* or Δ*Vdhog1* strains. In contrast to the phenotypes of the Δ*VdSsk2,* Δ*Vdpbs2*, Δ*Vdhog1*, the Δ*Vdste11* strain did not display any stress-sensitive phenotypes. It is well-known that hypersensitivity to high osmolarity and increased resistance to fludioxonil are two hallmarks of the Hog pathway and also appeared in the deletion mutants of Hog1 cascade components in other filamentous fungi, such as *Beauveria bassiana* (36), *Cochliobolus heterostrophus* (37), *Botrytis cinerea* (15), *Mycosphaerella graminicola* (17), *Colletotrichum lagenarium* (38), *Cryphonectria parasitica* (18), *Aspergillus nidulans* (39), and *Magnaporthe grisea* (19). More importantly, biochemical assays have demonstrated that Hog1 phosphorylation was inhibited in the absence of Ssk2, Pbs2, or Hog1, but not altered in the absence of Ste11, in response to high osmolarity (40, 41). This also supports the conclusion that VdSsk2, VdPbs2, and VdHog1 are sequentially phosphorylated in *V. dahliae* in response to hyperosmolarity, but not VdSte11. Taken together, in contrast to findings in model yeast systems, we propose that the Hog signaling occurs through sequential phosphorylation of the Ssk2, Pbs2, and Hog1 protein orthologs in filamentous fungi. However, it remains to be determined whether single or multiple histone kinases or other kinases function upstream of the cascade in response to various stressor cues. Using yeast two-hybrid assays, we found that neither VdSsk2 nor Ste11 physically interacts with VdPbs2 (data not shown). Exploring the biochemical and genetic connections between sensors, histone kinases, and the Hog pathway will be a future goal.

The budding yeast *S. cerevisiae* undergoes filamentous growth, which requires MAP kinase pathways (42). This seminal discovery led to knowledge that *S. cerevisiae* Ste11 is required for filamentous growth, whereas Ssk2/Ssk22 is not (43), which was consistent with our observations that the Δ*VdSte11* mutant was defective in filamentous growth while the Δ*VdSsk2* mutant had no obvious difference on filamentous growth.

The findings herein clarified distinctive roles of VdSsk2 and VdSte11 in the development of melanized microsclerotia in *V. dahliae*. Melanized microsclerotial formation is critically important in the life cycle of *V. dahliae* for both survival and spread (1). *Verticillium* virulence and the development of microsclerotia increasingly appear to be linked (44), though the basis for this correlation is not understood. Nevertheless, numerous genes have been characterized as having roles in the regulation of both virulence and microsclerotial development (44). Melanized microsclerotia produced by the fungus originate from hyphal swelling and septation, and then fungal cells within these clusters subsequently become dark due to melanin secretion (45, 46). In the present study, we provided several lines of evidence demonstrating distinctive functions of VdSsk2 and VdSte11 in microsclerotial formation and melanin biosynthesis. The Δ*VdSsk2* strain exhibited a severe delay in microsclerotial formation and melanization. Although the microsclerotial development of the Δ*Vdste11* strain was similar to that observed in the wild type, there was clearly a lack of melanin biosynthesis, suggesting that both VdSsk2 and VdSte11 are involved in melanization of the microsclerotia. Importantly, delayed and reduced melanized microsclerotial formation of the Δ*VdSsk2* strain mimics the phenotypes observed after deletion of multiple Hog1 MAPK pathway genes, including *VdHog1*, *VdPbs2*, *VdMsb,* and *VdSho1* (28–30, 34). Thus, mutation of *VdSsk2* or these components of the Hog MAPK pathway delays and reduces melanized microsclerotial formation in *V. dahliae*, demonstrating that the Hog pathway plays important roles in microsclerotial formation and melanization.

On the other hand, the Δ*VdSte11* strain exhibited a lack of melanin, especially during microsclerotial formation, which is reminiscent of the *vmk1* mutant (31). We also found that deletion of *VdSte7* does affect melanin biosynthesis, but not microsclerotial formation (not published), indicating that Ste11-Ste7-Kss1 functions as the MAPK cascade in *V. dahliae*. We also previously reported that VdCmr1 is required for melanin production, but not for microsclerotial development (5). In the current study, we demonstrated that expression of *VdCmr1* was significantly downregulated in the Δ*Vdste11* mutant. We further found that expression of most melanogenesis-associated genes, including that of *Vayg1,* was completely inhibited in the Δ*Vdste11* strain. Moreover, the transcription factor VdMsn2 was previously proven to be a negative

regulator of microsclerotial formation (27). The expression of VdMsn2 was upregulated in the Δ*Vdste11* mutant, which supports the observation of microsclerotial formation without melanin production. Taken together, these findings indicate that VdSte11 is required for melanin biosynthesis but not for microsclerotial development. However, melanin production was nevertheless impaired in Hog1 MAPK pathway mutants in culture, suggesting that melanogenesis is dependent on Hog1 signaling. It will be of interest to identify the overlapping mechanisms of melanogenesis regulated by different signaling pathways in future studies.

We also found that Ste11 plays a conserved role in pathogenesis in *V. dahliae*. Most pathogenic fungi possess infection-related MAPKs that are orthologs of the yeast Fus3/Kss1 MAPK, and these MAPKs play important functions in establishment of various infection strategies. Kss1 orthologs are essential for plant infection in many phytopathogens. For example, the *M. oryzae* PMK1 is crucial for appressorium formation and controls plant cell-to-cell invasion (47, 48). The genes upstream of PMK1, especially MAPKK MST7 and MAPKKK MST11, as well as the adaptor protein Ste50, are essential for differentiation of penetration structures and plant infection (49, 50). *M. oryzae* strains lacking *Ste11* failed to form appressoria and are nonpathogenic. In multiple pathogenic fungi, the deletion or disruption of *Ste11* resulted in the loss of virulence, i.e., *Colletotrichum orbiculare* (51), *Cochliobolus heterostrophus* (52), and *Candida albicans* (53). Indeed, the Ste11-Ste7-Kss1 cascade is required for infection in all phytopathogens examined (8, 54). The current studies show that deletion of *VdSte11* causes loss of pathogenicity, as the mutant fails to penetrate and develop invasive growth in *V. dahliae*.

Compared with *Magnaporthe oryzae*, very little is known about how the Ste11-Ste7-Kss1 cascade governs virulence and vascular colonization of *V. dahliae*. Disruption of *VdKss1* (previously known as *Vmk1*) resulted in reduced virulence against a variety of host plants (31). Furthermore, transcription factor Ste12 is a downstream target of the Ste11-Ste7-Kss1 cascade (55, 56). In *V. dahliae*, Vhb1, the Ste12 homolog, is required for virulence by impairing the ability to colonize the xylem (57). In agreement with these observations, the Δ*Vdste11* strain was avirulent. Significantly, our present study has highlighted the importance of studying this cascade in virulence of the soilborne fungus. Dissecting the specific roles of each of the VdSte11-VdSte7-VdKss1 cascade members in virulence requires further investigation.

This work focused on elucidating roles of *VdSsk2* and *VdSte11* in microsclerotial formation, stress responses, and pathogenicity. In doing so, we uncovered cross talk between the Hog cascade with other MAPK pathways in *V. dahliae*. Strikingly, the Δ*VdSsk2* mutant phenocopies the Δ*VdPbs2* and Δ*VdHog1* mutants under various stressors, the Δ*VdSte11* mutant had defects in filamentous growth, suggesting that in *V. dahliae*, there is an osmotic branch (VdSsk2-VdPbs2-VdHog1) and a filamentous branch (VdSte11). We noted that under high concentrations of $Ca^{2+}$, the strains lacking a functional Hog cascade (VdSsk2, VdPbs2, and VdHog1) were much more sensitive than the Δ*VdCrz1* strain. Crz1 is a key regulator of calcium signaling in fungi, and VdCrz1 plays important roles in $Ca^{2+}$ signaling and microsclerotia development in *V. dahliae* (32). Interestingly, consistent with the increased sensitivity of the mutants, the expression of *VdCrz1* was significantly downregulated in Hog cascade mutants. The results suggest that *VdCrz1* function is partly dependent on a functional Hog cascade, where the cascade directly influences *VdCrz1* gene expression induced by $Ca^{2+}$. We speculate that Vdcrz1 is regulated by the Hog cascade and $Ca^{2+}$ signaling. How VdCrz1 is regulated by the Hog pathway requires further analysis in *V. dahliae*. On the other hand, we also found that VdSsk2 and VdSte11 can coregulate several downstream target genes related to melanin biosynthesis, including the transcription factor VdCmr1 and the polyketide synthase (VdPKS1) (5). Similarly, in *C. heterostrophus*, Chk1 and Mps1 share multiple downstream targets, such as the transcription factor CMR1 and melanin biosynthetic genes (37). Taken together, we propose a simple model in Fig. 8 to account for the difference and convergence in the two MAPK pathways during micro-

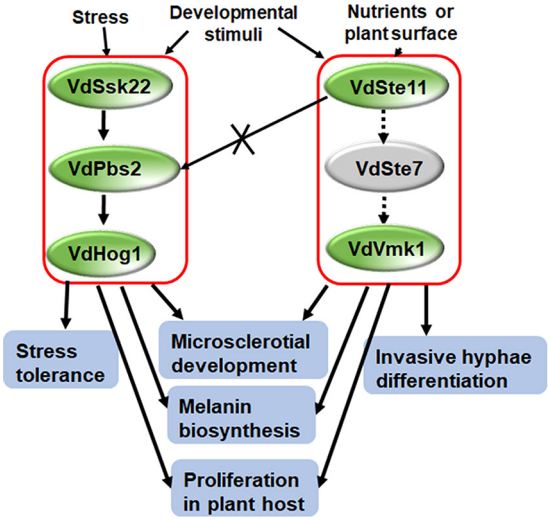


**FIG 8** A proposed model for the two MAPK pathways in *Verticillium dahliae*. Under osmotic stresses, the HOG cascade is activated, leading to an efficient stress response. The HOG cascade is also involved in melanized microsclerotial formation. Our phosphorylation assay demonstrated that a single VdSsk22 activates VdHog1, but not VdSte11, suggesting that the VdSte11 pathway does not transmit phosphorylation signals to the VdPbs2-VdHog1 module. During pathogenesis, the HOG cascade is important for proliferation but not for penetration. However, another MAPK cascade (Ste11-Ste7-Kss1 [Vmk1]) is required for penetration and differentiation of invasive hyphae. This Ste11-Ste7-Kss1 cascade is only required for regulating melanin biosynthesis during melanized microsclerotial formation.

sclerotial formation, stress response, and pathogenesis in *V. dahliae*, indicating that both pathways are distinct and converged.

In conclusion, the two MAPKKKs, VdSsk2 and VdSte11, play some distinctive roles in signaling for microsclerotial development, stress responses, and pathogenicity of *V. dahliae*. Our findings provide compelling evidence indicating that VdSsk2 is necessary for signaling through the VdPbs2-VdHog1 module, while VdSte11 is not necessary for this pathway. Although VdSsk2 (and the cognate Hog cascade) serves a more critical role as a regulator of fungal stress response, and VdSte11 plays a key role in the infection process, cross talk between MAPK cascades converged on microsclerotial development. With this framework, we are pursuing additional questions regarding the roles of MAPK pathways in *V. dahliae* for development, adaptation to surroundings, and pathogenesis. Characterization of the cross talk between MAPK cascades and other signaling pathways will lead to better understanding of the regulatory network involved in regulation of virulence and formation of microsclerotia as a resting structure of *V. dahliae*.

## MATERIALS AND METHODS

**Fungal strains and growth conditions.** The *Verticillium dahliae* strain XS11 (nondefoliating pathotype, race 2) was isolated from a smoke tree in Fragrant Hills Park, Beijing, China (58) and used as the parental strain to generate gene deletion mutants in this study. All the strain used in this study were primarily incubated on potato dextrose agar medium (PDA) (200 g potato, 20 g glucose, 15 g agar per liter). Conidia used for phenotypic analyses, including growth rate, yield and germination of conidia, and multistress assay, were acquired from a colony that was incubated for 7 days on PDA.

To observe microsclerotial formation, a conidial suspension of *V. dahliae* ($10^4$/ml) was sprayed onto a cellulose membrane (Ø = 80 mm; pore size = 0.22 $\mu$m), which was overlaid on solid basal medium (10 g glucose, 0.2 g/liter sodium nitrate, 0.52 g KCl, 0.52 g $MgSO_4 \cdot 7H_2O$, 1.52 g $KH_2PO_4$, l $\mu$M thiamine HCl, 0.1 $\mu$M biotin, 15 g agar per liter). In addition, the conidial suspension was incubated on glass slides that had been smeared with 500 $\mu$l solid basal medium (BM) (10 g glucose, 0.2 g sodium nitrate, 0.52 g KCl, 0.52 g $MgSO_4 \cdot 7H_2O$, 1.52 g $KH_2PO_4$, 3 $\mu$mol thiamine HCl, 0.1 mol biotin, and 15 g agar per liter). Microsclerotial formation was observed and photographed after incubation at 25°C at 48-h intervals. To test sensitivity to multiple stresses, including cell wall inhibitors, such as calcofluor white (CFW) (Sigma-Aldrich) and Congo red (CR) (Sigma-Aldrich), osmotic stresses, and fungicides, conidia of *V. dahliae* were incubated onto complete medium (CM) (50 ml of 20× nitrate salts, 1 ml of 1,000× trace element, 10 g glucose, 2 g peptone, 1 g yeast extract, 1 g Casamino Acids, 1 ml vitamin solution per liter)

described by M. J. Neumann and K. F. Dobinson (59) with or without 0.8 M and 1.0 M NaCl, 1.2 M and 1.4 M sorbitol, 0.4 M and 0.6 M $CaCl_2$, or 10 $\mu$g/ml and 30 $\mu$g/ml CFW, 25 $\mu$g/ml and 75 $\mu$g/ml CR at 25°C, respectively. To analyze the chitin distribution in the control and the Δ*VdSsk2* and Δ*VdSte11* strains, 20 $\mu$g/ml CFW was used for staining the hyphae in liquid yeast extract peptone-dextrose broth (YEPD) (3 g yeast extract, 10 g peptone, 20 g dextrose per liter) with or without 0.2 M NaCl for 3 days. Images were captured using a compound microscope (Leica DM 2500).

**Immunoblot analyses.** Total proteins were isolated from 48-h fresh mycelia grown in liquid CM cultures, separated on a 12.5% SDS-polyacrylamide gel. Separated total proteins were transferred to a nitrocellulose membrane, and the anti-phospho-p38 monoclonal antibody (P-Hog1; Cell Signaling) was used to detect the phosphorylated form of the *V. dahliae* Hog1p (VdHog1p). The same blots were stripped and then reprobed with a glyceraldehyde-3-phosphate dehydrogenase (GAPDH) antibody (catalog no. SRP00849; Saierbio) as the internal control.

**Bioinformatic analyses of VdSsk2 and VdSte11 with their homologs.** To identify orthologous genes *Ssk2* and *Ste11* in *V. dahliae*, the full-length amino acid sequences of ScSsk22 (YCR073C) and ScSte11p (YLR362W) were used in searches against the *V. dahliae* genome (60) with blastp (61). The homologs of Ssk2p and Ste11p in other fungi were searched with blastp at the National Center for Biotechnology Information (NCBI) database (https://www.ncbi.nlm.nih.gov). Phylogenetic trees were constructed by MEGA 6.0 (62) with the maximum likelihood algorithm under default settings and 1,000 bootstrap replications. Multiple sequence alignments were performed with ClustalX 2.0 (63).

**Deletion and complementation of *VdSsk2* and *VdSte11* in *V. dahliae*.** To delete *VdSsk2* and *VdSte11* in the genome of *V. dahliae* strain XS11, we used the split-marker method (64). All primers used were included in Table S1 in the supplemental material. The 5′ (1,329-bp) and 3′ (1,380-bp) flanking sequences of *VdSsk2* were amplified with primer pairs LY120/LY121 and LY158/LY159, respectively. The 5′ (972-bp) and 3′ (1,078-bp) flanking sequence of *VdSte11* were amplified with primer pairs LE9/LE13 and LE7/LE8, respectively. These flanking segments overlapped with Geneticin resistance cassette using primer pair Geneticinfor/Geneticinrev (for stands for forward, and rev stands for reverse). The deletion cassettes of *VdSsk2* were obtained with primer pairs LY120/Geneticinrev and Geneticinfor/LY159, and the deletion cassettes of *VdSte11* were obtained with primer pair LE9/Geneticinrev and Geneticinfor/LE8. Each of these products was verified by sequencing and then used for protoplast transformation in strain XS11. To obtain the *VdSsk2* complemented strain, a segment of DNA (5,951 bp) was amplified using primer pair LY119/LY124, which contain the native promoter and coding sequences of *VdSsk2*. To obtain the *VdSte11* complemented strain, the wild-type coding sequence of *VdSte11* was amplified with primer pairs LE9/LE6 (2,872 bp), and a fragment of DNA encoding an external promoter TrpC (464 bp) that was amplified from pRF-HU2 plasmid with primer pairs YJ104/YJ105, and both fragments were included in a final fusion PCR. The fusion products were transformed with the hygromycin resistance gene cassette into protoplasts of the Δ*VdSsk2* or Δ*VdSte11* deletion mutant by a polyethylene glycol (PEG) method (58). All transformants were verified with the external screening primers LY192/LY193 and the internal screening primers LY190/LY191.

**RNA extraction and quantitative real-time PCR.** For detection of the expression levels of genes with known roles in melanin biosynthesis and cell wall biogenesis, the mycelia of XS11, Δ*VdSsk2* and Δ*Vdste11* strains were collected after 7 days of incubation on PDA at 25°C. For calcium treatment, the mycelia of XS11, Δ*VdSsk2*, Δ*Vdpbs2*, Δ*Vdhog1*, and Δ*Vdcrz1* strains were incubated into liquid YEPD for 3 days, filtered, washed twice with water, and stimulated with 0.3 M $Ca^{2+}$ for 30 min for RNA extraction. Total RNA from the mycelia described above was extracted using TRIzol reagent (Invitrogen) and purified with an RNA minikit (Ambion). The cDNA from these strains was synthesized using SuperScript III reverse transcriptase (Invitrogen). Reverse transcription-quantitative PCR (RT-qPCR) was conducted with SYBR green (SuperReal-Premix Plus; Tiangen, China). All of these reactions were run on an ABI7500 real-time PCR system (Applied Biosystems, USA), and the agents for these assays were used in accordance with the manufacturer's instructions. The cycling conditions for the RT-qPCR experiments included an initial denaturation at 95°C for 15 min, followed by 40 cycles, with 1 cycle consisting of 95°C for 10 s and 60°C for 32 s. The results were calculated by the $2^{-\Delta\Delta CT}$ method (65). The *V. dahliae* $\beta$-tubulin gene was used as the internal reference for all RT-qPCR analyses by the method of Duressa et al. (7).

Nine genes used for RT-qPCR analyes were listed in Table 1. Four other genes included 1,3-$\beta$-glucan synthase (*VDAG_02340* and *VDAG_02341*), glucan synthesis regulatory protein (*VDAG_08428*), and *VdCrz1* (*VDAG_03208*). All primers used for these analyses are listed in Table S1.

**Pathogenicity and penetration assays.** Pathogenicity assays were performed in greenhouses with tobacco seedlings using a root dip method as previously reported by D. Xiong et al. (66). Conidia were filtered from liquid CM after 8 days of incubation and diluted to $2 \times 10^6$/ml with distilled water. Three-month-old tobacco seedlings were washed briefly in tap water, soaked in the conidial suspension for 10 min, and replanted into autoclaved soil. The observations for pathogenicity experiments were performed at every 5 days postinoculation (dpi). To determine the ability of strains to approach the vascular system in tobacco, at 5 weeks postinoculation, stem sections around above 10 cm soil were collected and placed on PDA medium. PDA plates were incubated at 25°C for 7 days for observing *V. dahliae* colonies. The fungal colonies were then transferred to fresh PDA for another 10 days for imaging. The experiment was repeated three times with four replicates.

To observe the ability of the *V. dahliae* strains to penetrate onion epidermis membrane and cellophane membrane, conidiospores of *VdSsk2* and *VdSte11* deletion strains were collected from PDA after 7 days of incubation, diluted to $10^4$/ml with sterile water, and inoculated onto each surface at 25°C. Observations of hyphopodia and penetration pegs were performed, and images were captured using a compound microscope (Leica DM 2500) at 24-h intervals.

## SUPPLEMENTAL MATERIAL

Supplemental material for this article may be found at https://doi.org/10.1128/mSphere.00426-19.

**FIG S1**, TIF file, 2.4 MB.
**FIG S2**, TIF file, 2.4 MB.
**FIG S3**, TIF file, 1.8 MB.
**FIG S4**, TIF file, 2.3 MB.
**FIG S5**, TIF file, 2.5 MB.
**TABLE S1**, DOCX file, 0.02 MB.

## ACKNOWLEDGMENTS

The research was supported by Key Project of National Key Research and Development Plan (2018YFD0600200) and the National Natural Science Foundation of China (31570636).

Y. Wang conceived the experiments. J. Yu, T. Li, L. Tian, and C. Tang performed the experiments. J. Yu, L. Tian, Y. Wang, and C. Tian analyzed the data. Y. Wang and S. J. Klosterman wrote the manuscript. All authors read and approved the manuscript.

## REFERENCES

1. Klosterman SJ, Atallah ZK, Vallad GE, Subbarao KV. 2009. Diversity, pathogenicity, and management of Verticillium species. Annu Rev Phytopathol 47:39–62. https://doi.org/10.1146/annurev-phyto-080508-081748.
2. Vallad GE, Subbarao KV. 2008. Colonization of resistant and susceptible lettuce cultivars by a green fluorescent protein-tagged isolate of *Verticillium dahliae*. Phytopathology 98:871–885. https://doi.org/10.1094/PHYTO-98-8-0871.
3. Klimes A, Dobinson KF. 2006. A hydrophobin gene, VDH1, is involved in microsclerotial development and spore viability in the plant pathogen *Verticillium dahliae*. Fungal Genet Biol 43:283–294. https://doi.org/10.1016/j.fgb.2005.12.006.
4. Xiong D, Wang Y, Ma J, Klosterman SJ, Xiao S, Tian C. 2014. Deep mRNA sequencing reveals stage-specific transcriptome alterations during microsclerotia development in the smoke tree vascular wilt pathogen, *Verticillium dahliae*. BMC Genomics 15:324. https://doi.org/10.1186/1471-2164-15-324.
5. Wang Y, Hu X, Fang Y, Anchieta A, Goldman PH, Hernandez G, Klosterman SJ. 2018. Transcription factor VdCmr1 is required for pigment production, protection from UV irradiation, and regulates expression of melanin biosynthetic genes in *Verticillium dahliae*. Microbiology 164:685–696. https://doi.org/10.1099/mic.0.000633.
6. Bell AA, Wheeler MH. 1986. Biosynthesis and functions of fungal melanins. Annu Rev Phytopathol 24:411–451. https://doi.org/10.1146/annurev.py.24.090186.002211.
7. Duressa D, Anchieta A, Chen D, Klimes A, Garcia-Pedrajas MD, Dobinson KF, Klosterman SJ. 2013. RNA-seq analyses of gene expression in the microsclerotia of *Verticillium dahliae*. BMC Genomics 14:607. https://doi.org/10.1186/1471-2164-14-607.
8. Turra D, Segorbe D, Di Pietro A. 2014. Protein kinases in plant-pathogenic fungi: conserved regulators of infection. Annu Rev Phytopathol 52:267–288. https://doi.org/10.1146/annurev-phyto-102313-050143.
9. Hamel LP, Nicole MC, Duplessis S, Ellis BE. 2012. Mitogen-activated protein kinase signaling in plant-interacting fungi: distinct messages from conserved messengers. Plant Cell 24:1327–1351. https://doi.org/10.1105/tpc.112.096156.
10. Banuett F. 1998. Signalling in the yeasts: an informational cascade with links to the filamentous fungi. Microbiol Mol Biol Rev 62:249–274.
11. Maeda T, Takekawa M, Saito H. 1995. Activation of yeast PBS2 MAPKK by MAPKKKs or by binding of an SH3-containing osmosensor. Science 269:554–558. https://doi.org/10.1126/science.7624781.
12. Posas F, Wurgler-Murphy SM, Maeda T, Witten EA, Thai TC, Saito H. 1996. Yeast HOG1 MAP kinase cascade is regulated by a multistep phosphorelay mechanism in the SLN1-YPD1-SSK1 "two-component" osmosensor. Cell 86:865–875. https://doi.org/10.1016/S0092-8674(00)80162-2.
13. Gustin MC, Albertyn J, Alexander M, Davenport K. 1998. MAP kinase pathways in the yeast *Saccharomyces cerevisiae*. Microbiol Mol Biol Rev 62:1264–1300.
14. Li A, Wang Y, Tao K, Dong S, Huang Q, Dai T, Zheng X, Wang Y. 2010. PsSAK1, a stress-activated MAP kinase of *Phytophthora sojae*, is required for zoospore viability and infection of soybean. Mol Plant Microbe Interact 23:1022–1031. https://doi.org/10.1094/MPMI-23-8-1022.
15. Segmuller N, Ellendorf U, Tudzynski B, Tudzynski P. 2007. BcSAK1, a stress-activated mitogen-activated protein kinase, is involved in vegetative differentiation and pathogenicity in *Botrytis cinerea*. Eukaryot Cell 6:211–221. https://doi.org/10.1128/EC.00153-06.
16. Moriwaki A, Kubo E, Arase S, Kihara J. 2006. Disruption of SRM1, a mitogen-activated protein kinase gene, affects sensitivity to osmotic and ultraviolet stressors in the phytopathogenic fungus *Bipolaris oryzae*. FEMS Microbiol Lett 257:253–261. https://doi.org/10.1111/j.1574-6968.2006.00178.x.
17. Mehrabi R, Zwiers LH, de Waard MA, Kema GH. 2006. MgHog1 regulates dimorphism and pathogenicity in the fungal wheat pathogen *Mycosphaerella graminicola*. Mol Plant Microbe Interact 19:1262–1269. https://doi.org/10.1094/MPMI-19-1262.
18. Park SM, Choi ES, Kim MJ, Cha BJ, Yang MS, Kim DH. 2004. Characterization of HOG1 homologue, CpMK1, from *Cryphonectria parasitica* and evidence for hypovirus-mediated perturbation of its phosphorylation in response to hypertonic stress. Mol Microbiol 51:1267–1277. https://doi.org/10.1111/j.1365-2958.2004.03919.x.
19. Dixon KP, Xu JR, Smirnoff N, Talbot NJ. 1999. Independent signaling pathways regulate cellular turgor during hyperosmotic stress and appressorium-mediated plant infection by *Magnaporthe grisea*. Plant Cell 11:2045–2058. https://doi.org/10.1105/tpc.11.10.2045.
20. Wang C, Zhang S, Hou R, Zhao Z, Zheng Q, Xu Q, Zheng D, Wang G, Liu H, Gao X, Ma JW, Kistler HC, Kang Z, Xu JR. 2011. Functional analysis of the kinome of the wheat scab fungus *Fusarium graminearum*. PLoS Pathog 7:e1002460. https://doi.org/10.1371/journal.ppat.1002460.
21. Berridge MJ, Bootman MD, Roderick HL. 2003. Calcium signalling: dynamics, homeostasis and remodelling. Nat Rev Mol Cell Biol 4:517–529. https://doi.org/10.1038/nrm1155.
22. Chin D, Means AR. 2000. Calmodulin: a prototypical calcium sensor. Trends Cell Biol 10:322–328. https://doi.org/10.1016/S0962-8924(00)01800-6.
23. Stathopoulos AM, Cyert MS. 1997. Calcineurin acts through the CRZ1/TCN1-encoded transcription factor to regulate gene expression in yeast. Genes Dev 11:3432–3444. https://doi.org/10.1101/gad.11.24.3432.
24. Choi J, Kim Y, Kim S, Park J, Lee YH. 2009. MoCRZ1, a gene encoding a calcineurin-responsive transcription factor, regulates fungal growth and pathogenicity of *Magnaporthe oryzae*. Fungal Genet Biol 46:243–254. https://doi.org/10.1016/j.fgb.2008.11.010.
25. Zhang H, Zhao Q, Liu K, Zhang Z, Wang Y, Zheng X. 2009. MgCRZ1, a transcription factor of *Magnaporthe grisea*, controls growth, development and is involved in full virulence. FEMS Microbiol Lett 293:160–169. https://doi.org/10.1111/j.1574-6968.2009.01524.x.
26. Schumacher J, de Larrinoa IF, Tudzynski B. 2008. Calcineurin-responsive

zinc finger transcription factor CRZ1 of *Botrytis cinerea* is required for growth, development, and full virulence on bean plants. Eukaryot Cell 7:584–601. https://doi.org/10.1128/EC.00426-07.
27. Tian L, Yu J, Wang Y, Tian C. 2017. The $C_2H_2$ transcription factor VdMsn2 controls hyphal growth, microsclerotia formation, and virulence of *Verticillium dahliae*. Fungal Biol 121:1001–1010. https://doi.org/10.1016/j.funbio.2017.08.005.
28. Wang Y, Tian L, Xiong D, Klosterman SJ, Xiao S, Tian C. 2016. The mitogen-activated protein kinase gene, VdHog1, regulates osmotic stress response, microsclerotia formation and virulence in *Verticillium dahliae*. Fungal Genet Biol 88:13–23. https://doi.org/10.1016/j.fgb.2016.01.011.
29. Tian L, Wang Y, Yu J, Xiong D, Zhao H, Tian C. 2016. The mitogen-activated protein kinase kinase VdPbs2 of *Verticillium dahliae* regulates microsclerotia formation, stress response, and plant infection. Front Microbiol 7:1532. https://doi.org/10.3389/fmicb.2016.01532.
30. Qi XY, Zhou S, Shang XG, Wang XY. 2016. VdSho1 regulates growth, oxidant adaptation and virulence in *Verticillium dahliae*. J Phytopathol 164:1064–1074. https://doi.org/10.1111/jph.12527.
31. Rauyaree P, Ospina-Giraldo MD, Kang S, Bhat RG, Subbarao KV, Grant SJ, Dobinson KF. 2005. Mutations in VMK1, a mitogen-activated protein kinase gene, affect microsclerotia formation and pathogenicity in *Verticillium dahliae*. Curr Genet 48:109–116. https://doi.org/10.1007/s00294-005-0586-0.
32. Xiong D, Wang Y, Tang C, Fang Y, Zou J, Tian C. 2015. VdCrz1 is involved in microsclerotia formation and required for full virulence in *Verticillium dahliae*. Fungal Genet Biol 82:201–212. https://doi.org/10.1016/j.fgb.2015.07.011.
33. Madhani HD, Styles CA, Fink GR. 1997. MAP kinases with distinct inhibitory functions impart signaling specificity during yeast differentiation. Cell 91:673–684. https://doi.org/10.1016/S0092-8674(00)80454-7.
34. Tian L, Xu J, Zhou L, Guo W. 2014. VdMsb regulates virulence and microsclerotia production in the fungal plant pathogen *Verticillium dahliae*. Gene 550:238–244. https://doi.org/10.1016/j.gene.2014.08.035.
35. Ha YS, Covert SF, Momany M. 2006. FsFKS1, the 1,3-beta-glucan synthase from the caspofungin-resistant fungus *Fusarium solani*. Eukaryot Cell 5:1036–1042. https://doi.org/10.1128/EC.00030-06.
36. Liu J, Wang ZK, Sun HH, Ying SH, Feng MG. 2017. Characterization of the Hog1 MAPK pathway in the entomopathogenic fungus *Beauveria bassiana*. Environ Microbiol 19:1808–1821. https://doi.org/10.1111/1462-2920.13671.
37. Igbaria A, Lev S, Rose MS, Lee BN, Hadar R, Degani O, Horwitz BA. 2008. Distinct and combined roles of the MAP kinases of *Cochliobolus heterostrophus* in virulence and stress responses. Mol Plant Microbe Interact 21:769–780. https://doi.org/10.1094/MPMI-21-6-0769.
38. Kojima K, Takano Y, Yoshimi A, Tanaka C, Kikuchi T, Okuno T. 2004. Fungicide activity through activation of a fungal signalling pathway. Mol Microbiol 53:1785–1796. https://doi.org/10.1111/j.1365-2958.2004.04244.x.
39. Kawasaki L, Sanchez O, Shiozaki K, Aguirre J. 2002. SakA MAP kinase is involved in stress signal transduction, sexual development and spore viability in *Aspergillus nidulans*. Mol Microbiol 45:1153–1163. https://doi.org/10.1046/j.1365-2958.2002.03087.x.
40. Noguchi R, Banno S, Ichikawa R, Fukumori F, Ichiishi A, Kimura M, Yamaguchi I, Fujimura M. 2007. Identification of OS-2 MAP kinase-dependent genes induced in response to osmotic stress, antifungal agent fludioxonil, and heat shock in *Neurospora crassa*. Fungal Genet Biol 44:208–218. https://doi.org/10.1016/j.fgb.2006.08.003.
41. Lee YM, Kim E, An J, Lee Y, Choi E, Choi W, Moon E, Kim W. 2017. Dissection of the HOG pathway activated by hydrogen peroxide in *Saccharomyces cerevisiae*. Environ Microbiol 19:584–597. https://doi.org/10.1111/1462-2920.13499.
42. Gimeno CJ, Ljungdahl PO, Styles CA, Fink GR. 1992. Unipolar cell divisions in the yeast *S. cerevisiae* lead to filamentous growth: regulation by starvation and RAS. Cell 68:1077–1090. https://doi.org/10.1016/0092-8674(92)90079-R.
43. Roberts RL, Fink GR. 1994. Elements of a single MAP kinase cascade in Saccharomyces cerevisiae mediate two developmental programs in the same cell type: mating and invasive growth. Genes Dev 8:2974–2985. https://doi.org/10.1101/gad.8.24.2974.
44. Klimes A, Dobinson KF, Thomma BP, Klosterman SJ. 2015. Genomics spurs rapid advances in our understanding of the biology of vascular wilt pathogens in the genus Verticillium. Annu Rev Phytopathol 53:181–198. https://doi.org/10.1146/annurev-phyto-080614-120224.
45. Griffiths DA. 1970. The fine structure of developing microsclerotia of *Verticillium dahliae* Kleb. Archiv Mikrobiol 74:207–212. https://doi.org/10.1007/BF00408881.
46. Coley-Smith JR, Cooke RC. 1971. Survival and germination of fungal sclerotia. Annu Rev Phytopathol 9:65–92. https://doi.org/10.1146/annurev.py.09.090171.000433.
47. Sakulkoo W, Oses-Ruiz M, Oliveira Garcia E, Soanes DM, Littlejohn GR, Hacker C, Correia A, Valent B, Talbot NJ. 2018. A single fungal MAP kinase controls plant cell-to-cell invasion by the rice blast fungus. Science 359:1399–1403. https://doi.org/10.1126/science.aaq0892.
48. Xu JR, Hamer JE. 1996. MAP kinase and cAMP signaling regulate infection structure formation and pathogenic growth in the rice blast fungus *Magnaporthe grisea*. Genes Dev 10:2696–2706. https://doi.org/10.1101/gad.10.21.2696.
49. Zhao X, Kim Y, Park G, Xu J. 2005. A mitogen-activated protein kinase cascade regulating infection-related morphogenesis in *Magnaporthe grisea*. Plant Cell 17:1317–1329. https://doi.org/10.1105/tpc.104.029116.
50. Park G, Xue C, Zhao X, Kim Y, Orbach M, Xu JR. 2006. Multiple upstream signals converge on the adaptor protein Mst50 in *Magnaporthe grisea*. Plant Cell 18:2822–2835. https://doi.org/10.1105/tpc.105.038422.
51. Sakaguchi A, Tsuji G, Kubo Y. 2010. A yeast STE11 homologue CoMEKK1 is essential for pathogenesis-related morphogenesis in *Colletotrichum orbiculare*. Mol Plant Microbe Interact 23:1563–1572. https://doi.org/10.1094/MPMI-03-10-0051.
52. Izumitsu K, Yoshimi A, Kubo D, Morita A, Saitoh Y, Tanaka C. 2009. The MAPKK kinase ChSte11 regulates sexual/asexual development, melanization, pathogenicity, and adaptation to oxidative stress in *Cochliobolus heterostrophus*. Curr Genet 55:439–448. https://doi.org/10.1007/s00294-009-0257-7.
53. Csank C, Schroppel K, Leberer E, Harcus D, Mohamed O, Meloche S, Thomas DY, Whiteway M. 1998. Roles of the Candida albicans mitogen-activated protein kinase homolog, Cek1p, in hyphal development and systemic candidiasis. Infect Immun 66:2713–2721.
54. Jiang C, Zhang X, Liu H, Xu JR. 2018. Mitogen-activated protein kinase signaling in plant pathogenic fungi. PLoS Pathog 14:e1006875. https://doi.org/10.1371/journal.ppat.1006875.
55. Rispail N, Di Pietro A. 2010. The homeodomain transcription factor Ste12: connecting fungal MAPK signalling to plant pathogenicity. Commun Integr Biol 3:327–332. https://doi.org/10.4161/cib.3.4.11908.
56. Elion EA, Qi M, Chen W. 2005. Signaling specificity in yeast. Science 307:687–688. https://doi.org/10.1126/science.1109500.
57. Sarmiento-Villamil JL, Prieto P, Klosterman SJ, García-Pedrajas MD. 2018. Characterization of two homeodomain transcription factors with critical but distinct roles in virulence in the vascular pathogen *Verticillium dahliae*. Mol Plant Pathol 19:986–1004. https://doi.org/10.1111/mpp.12584.
58. Wang Y, Xiao S, Xiong D, Tian C. 2013. Genetic transformation, infection process and qPCR quantification of *Verticillium dahliae* on smoke-tree *Cotinus coggygria*. Australas Plant Pathol 42:33–41. https://doi.org/10.1007/s13313-012-0172-0.
59. Neumann MJ, Dobinson KF. 2003. Sequence tag analysis of gene expression during pathogenic growth and microsclerotia development in the vascular wilt pathogen *Verticillium dahliae*. Fungal Genet Biol 38:54–62. https://doi.org/10.1016/S1087-1845(02)00507-8.
60. Klosterman SJ, Subbarao KV, Kang SC, Veronese P, Gold SE, Thomma B, Chen ZH, Henrissat B, Lee YH, Park J, Garcia-Pedrajas MD, Barbara DJ, Anchieta A, de Jonge R, Santhanam P, Maruthachalam K, Atallah Z, Amyotte SG, Paz Z, Inderbitzin P, Hayes RJ, Heiman DI, Young S, Zeng QD, Engels R, Galagan J, Cuomo CA, Dobinson KF, Ma LJ. 2011. Comparative genomics yields insights into niche adaptation of plant vascular wilt pathogens. PLoS Pathog 7:e1002137. https://doi.org/10.1371/journal.ppat.1002137.
61. Altschul SF, Gish W, Miller W, Myers EW, Lipman DJ. 1990. Basic local alignment search tool. J Mol Biol 215:403–410. https://doi.org/10.1016/S0022-2836(05)80360-2.
62. Tamura K, Stecher G, Peterson D, Filipski A, Kumar S. 2013. MEGA6: Molecular Evolutionary Genetics Analysis version 6.0. Mol Biol Evol 30:2725–2729. https://doi.org/10.1093/molbev/mst197.
63. Larkin MA, Blackshields G, Brown NP, Chenna R, McGettigan PA, McWilliam H, Valentin F, Wallace IM, Wilm A, Lopez R, Thompson JD, Gibson TJ, Higgins DG. 2007. Clustal W and Clustal X version 2.0. Bioinformatics 23:2947–2948. https://doi.org/10.1093/bioinformatics/btm404.

64. Goswami RS. 2012. Targeted gene replacement in fungi using a split-marker approach. Methods Mol Biol 835:255–269. https://doi.org/10.1007/978-1-61779-501-5_16.
65. Livak KJ, Schmittgen TD. 2001. Analysis of relative gene expression data using real-time quantitative PCR and the $2^{-\Delta\Delta CT}$ method. Methods 25:402–408. https://doi.org/10.1006/meth.2001.1262.
66. Xiong D, Wang Y, Tian L, Tian C. 2016. MADS-box transcription factor VdMcm1 regulates conidiation, microsclerotia formation, pathogenicity, and secondary metabolism of *Verticillium dahliae*. Front Microbiol 7:1192. https://doi.org/10.3389/fmicb.2016.01192.
67. Fan R, Klosterman SJ, Wang C, Subbarao KV, Xu X, Shang W, Hu X. 2017. Vayg1 is required for microsclerotium formation and melanin production in Verticillium dahliae. Fungal Genet Biol 98:1–11. https://doi.org/10.1016/j.fgb.2016.11.003.